STANFORD UNIVERSITY

Thermodynamic Optimization of Retinal Photocoagulation Surgery

Computational Model with Experimental Verification

Jefferson Brown

Research Advisor: Daniel Palanker (Ophthalmology)

Second Reader: Sarah Church (Physics)

5/8/2010

Abstract: Current safety considerations in retinal laser photocoagulation limit the exposure duration to a minimum of 20 ms per pulse. By numerical thermal modeling verified by *in vivo* experiments with 22 Dutch Belted rabbits, we demonstrate that this procedure can be rendered safe at pulse durations as short as 10 ms by spatial or temporal profile shaping of the laser beam. A combined spatio-temporal modulation may further decrease the minimal duration to 5 ms. Along with decreasing operation time, this increase of speed is expected to decrease the heat diffusion into the inner retina and choroid, therefore reducing the pain and discomfort for the patient, as well as decreasing collateral damage to the inner retina.

Table of Contents

Acknowledgment

This research summarizes the results of a group study from 2008-2010, under the direction of Professor Daniel Palanker. The work has been submitted (April 2010) as two companion papers to the Journal of Biomedical Optics under the following references:

Enhancing safety of retinal photocoagulation by modulation of laser power

Christopher Sramek[1], Loh-Shan Leung[2], Jefferson Brown[3], Theodore Leng[2], Georg Schuele[4], Daniel Palanker[2,5]

Enhancing safety of retinal photocoagulation by shaping the laser beam

Christopher Sramek[1], Loh-Shan Leung[2], Theodore Leng[2], Yannis Paulus[2], Jefferson Brown[3], Daniel Palanker[2,5]

[1] Department of Applied Physics, Stanford University, Stanford, CA

[2] Department of Ophthalmology, Stanford University, Stanford, CA

[3] Department of Physics, Stanford University, Stanford, CA

[4] OptiMedica Corp., Santa Clara, CA

[5] Hansen Experimental Physics Laboratory, Stanford University, Stanford, CA

Funding for this research has been provided by the Stanford Physics Department Summer Research Grants, Stanford UAR Major Grants, US Air Force Office of Scientific Research (FA9550-04-1-0075) and Stanford Photonics Research Center.

Thanks to Ilya Toytman for laser advice, Alex Chang for laboratory support and help with software development for pulse shaping, Nicholas Henderson for discussions on optimization methodology, Ryan Tibshirani for guidance with the statistical analysis, Hiroyuki Nomoto for help with animal handling, Roopa Dalal for histological preparations, and Georg Schuele for assistance with PASCAL. All images courtesy Christopher Sramek.

A special thanks also to Daniel Palanker and Christopher Sramek for their mentorship.

1. Introduction

Lasers have been employed in retinal photocoagulation surgery since 1964[1], and the procedure is still widely used today as a result of its observed clinical efficacy in treating such retinal disorders as diabetic retinopathy and macular degeneration, the two most common causes of blindness in developed countries[2]. The therapeutic mechanism of retinal photocoagulation operates upon laser deposition of heat into the melanin found in the thin layer of closely packed retinal pigmented epithelium (RPE) cells (Figure 1), which has a high absorption coefficient for visible wavelengths.

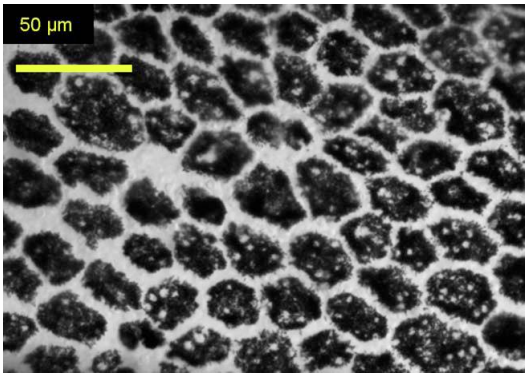

Figure 1. Transmittance micrograph of rabbit RPE sheet taken at 563-nm wavelength.

For laser radiation of 532-nm (green) wavelength, approximately 50% of the incident radiation is absorbed by the 4-µm thick RPE layer in humans, while most of the other 50% is diffusely absorbed by hemoglobin and melanin in the 70-µm thick choroid[3]. Since the RPE is located in close contact with the photoreceptor layer of the retina (Figure 2), concentrated hyperthermia at the RPE can selectively damage a region of photoreceptors as needed by the ophthalmologist to treat retinopathy.

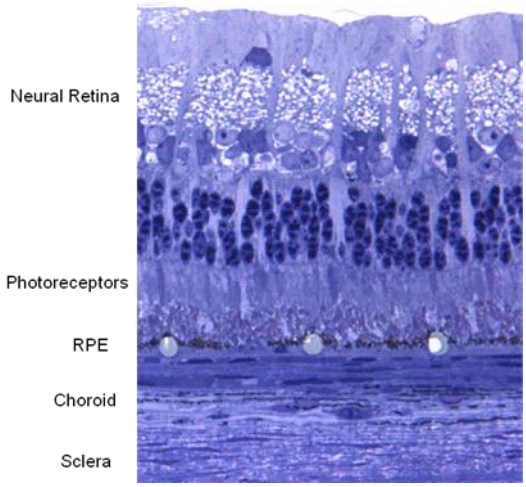

Figure 2. Histological cross-section of the retinal layers. The RPE is the thin (~4 µm) dark layer resting between the photoreceptor layer and the choroid.

To minimize pain, discomfort, and long-term retinal scarring in the patient, it is desirable to minimize damage to surrounding tissue layers beyond the photoreceptor layer. Shorter durations of each applied laser pulse can accomplish this by confining heat diffusion to a more localized region, as discussed in section 2.1 below. If heat can be confined to a thinner layer, pain-signaling neurons in the choroid will be less likely to fire, and fewer layers of tissue will experience thermal damage.

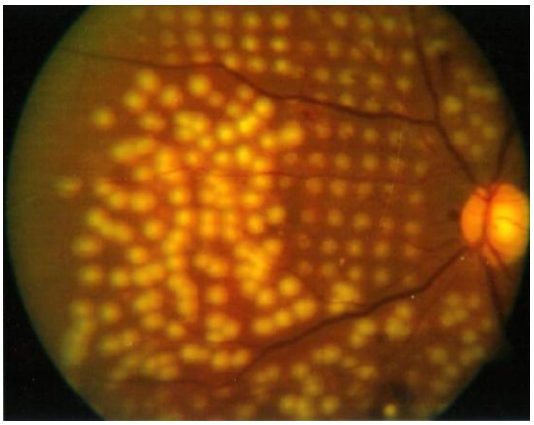

Figure 3. Pan-retinal photocoagulation in treatment of diabetic retinopathy: on the left are conventional lesions placed individually, on the right are grids of lesions placed by the PASCAL system.

A further advantage to short pulse durations is seen in the recent development by the Palanker group of the Patterned Scanning Laser (PASCAL) surgical suite, in which user-defined grids of up to 25 exposures are delivered in quick succession by a computer-controlled scanning mirror (Figure 3). This greatly lessens the time of the overall surgery, in which hundreds of lesions are typically applied[4]. The number of gridded lesions possible to fit in a single pulse is limited by the blink reflex of the eye, which is about 500 ms. Shorter pulse durations would allow more lesions to fit within this time constraint, reducing the overall time of surgery.

However, shorter pulse durations also require higher applied power to achieve the same clinical result, which increases the risk of photomechanical injury by water vaporization. If a localized region around the RPE is heated sufficiently to vaporize water, a rapidly expanding microbubble can form in the retinal layers. This can rupture Bruch's membrane between the RPE and the choroid, causing painful hemorrhage (bleeding) in the eye and permanent retinal scarring.

The need to control the safety of photocoagulation surgery leads to definition of a safety metric termed the "therapeutic window" (TW) of operation, defined as the ratio of the minimum laser power required to produce a rupture event over the minimum power required to produce a clinically effective lesion. Experimental threshold power measurements for determining TW (Figure 4) demonstrate a ratio that decreases with laser pulse duration, with a value approaching unity at the 1-ms duration.

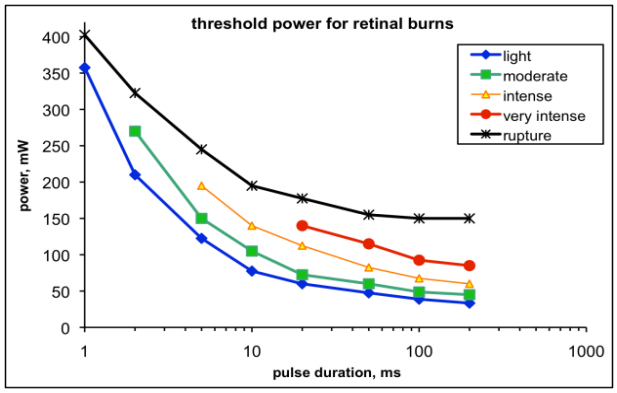

Figure 4. Threshold laser power required to produce various intensities of retinal lesions using a conventional laser beam. The therapeutic window is the power ratio of the top and bottom thresholds.

An optimum regime would maximize speed of treatment while maintaining a TW of at

least 3, as the relative concentration of melanin in human retinas is reported[5,6] to vary from one patient to another by up to a factor of 2, and pigmentation within a single eye has also been reported[7] to vary between the periphery and fundus by up to a factor of 3. This constraint limits current techniques to pulse durations of 20 ms or longer[8].

Gerstman et al. demonstrated that for exposures longer than approximately 10 μs, the mechanism of cell death is mainly thermal, rather than mechanical or photochemical[9]. Since we are limited by safety constraints to pulse durations longer than 20 ms, we are well above this 10-μs transition and can be confident that we are operating in the thermal damage regime.

In this study, we applied a computational thermal model to predict methods of improving the control of thermal damage during photocoagulation surgery. Based on this, we investigated two modifications to the applied laser radiation: spatial shaping and temporal shaping, both of which were expected to improve the dynamic temperature profile of the targeted tissue region. This we measured by testing improvement in TW values for pulse durations ranging from 5-20 ms for the temporally modulated pulses, and from 2-50 ms for the spatially shaped laser beams.

2. Computational Model

Because the surgical damage incurred in the tens of milliseconds pulse duration range is mainly thermal, computer-assisted thermal modeling can aid in assessing clinical effectiveness of arbitrary treatment regimes. Sramek et al. developed a finite-element numerical model of the retina employing the Arrhenius cell death scenario to predict extent of damage by hyperthermia from an arbitrarily shaped laser source, which has been shown to closely match histological data for laser pulses of various intensities and durations[10].

2.1 *Heat Diffusion*

The thermal response to a heat source is governed by the three-dimensional heat equation[11]:

$$\frac{\partial}{\partial t}u(\vec{r},t) - \kappa\nabla^2 u(\vec{r},t) = f(\vec{r},t) \quad (1)$$

where $u(r,t)$ is the temperature, f is a function defining the heat source, and κ is the thermal diffusivity of the region in question. In the case of retinal absorption of laser radiation, the problem can be modeled as that of a thin-disk heat source inside a 3-dimensional space with a nearly constant thermal diffusivity comparable to that of water (Figure 5). Inclusion of a central "hotspot" representing an especially

dense clustering of melanosomes within the absorbing RPE layer was shown in the Sramek model to improve the accuracy of the model's therapeutic window predictions in comparison with experimental observations.

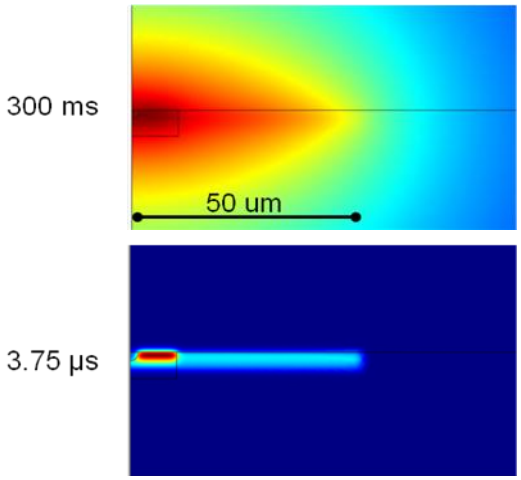

Figure 5. Heat diffusion model for flat disk heating with central hotspot at 300-ms and 3.75-µs pulse durations. Radial symmetry is implied.

Solutions to the heat equation universally exhibit heat flowing sharply down the temperature gradient over time. In the case of the given model, this means that at longer time scales, the heat will penetrate deeply until an almost spherical steady state is reached, while very short time scales will confine the heat essentially to the 2-dimensional disk where it is initially absorbed.

2.2 *Arrhenius Approximation of Cellular Toxicity*

The Arrhenius model of cell death operates on the following three assumptions[12,13]: (a) there exists some component in the cell critical to cell survival which can be thermally denatured, (b) this denaturing reaction can be described in terms of chemical theory, and (c) the rate of internal cell repair is insignificant during the duration of the incurred damage (in this case, the laser pulse). If these assumptions hold, this thermal denaturing is then approximated[12] by the following integral expression:

$$\Omega = A \int_0^{\tau} \exp\left[-\frac{E^*}{RT(t)}\right] dt, \quad (2)$$

where Ω is the cell damage threshold (by convention, regions where this value reaches 1 causes cell death[14]), τ is the duration of hyperthermia, $T(t)$ is the absolute temperature at time t (in Kelvin), and R is the gas constant (8.314 J/mol K). A (the reaction rate constant in 1/sec) and E^* (the activation energy in J/mol) are experimentally determined parameters of the tissue in question. For our purposes, it is sufficient to note that the rate of thermal damage incurred is an exponential function of T. Because of this, the extent of cell damage is highly sensitive to even small adjustments to the way heat is deposited in the tissue. Differences of only a few degrees in the time-integrated peak temperature rise can be sufficient in

determining whether a retinal burn is light, intense, or causes rupture (cf. Figure 7 below).

The main objectives, then, in devising a safer thermodynamic profile are to find ways of controlling a sustained temperature rise in the targeted regions while minimizing heat diffusion to non-targeted tissue, and to also minimize overheating of any particular region to diminish excess damage. This should maintain or reduce the power required to produce a minimal lesion and increase the power required to produce a rupture event, thus increasing the therapeutic window from both ends of the ratio.

2.3 *Spatial Shaping: Ring Beam*

During conventional laser exposures on a homogenous absorbing layer using a beam with a top-hat-shaped radial profile, the temperature gradient is most pronounced at the edges of the targeted spot, causing heat to diffuse more rapidly from the edges than from the center. This causes a temperature spike in the center of the targeted treatment zone (Figure 6a). A ring-shaped beam compensates for this by sourcing less heat into the center, resulting in a more even heat distribution (Figures 6b, 6c).

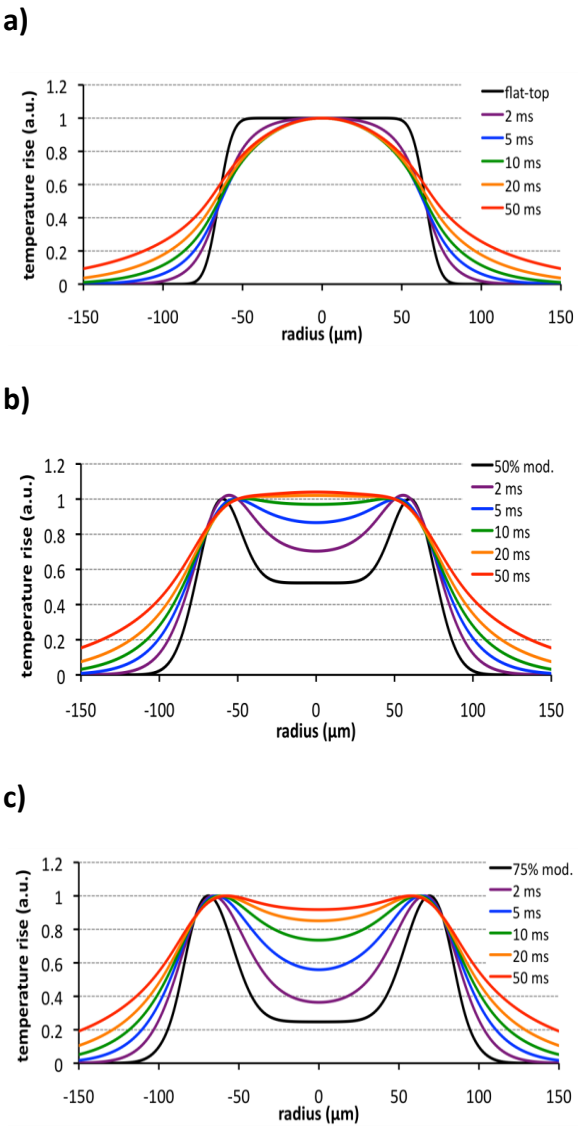

Figure 6. Spatial optimization: computed temperature profiles for a beam (black line) with (a) no radial modulation ("top hat" shape), (b) 50% modulation, and (c) 75% modulation. Profiles computed for durations 2-50 ms.

Depending on the pulse duration, different levels of modulation from the center to the edges may be optimal, as the level of heat diffusion is time-dependent. For example, the model used here predicted that 75% modulation should be optimal at the 10-ms duration, while

50% modulation should give a safer pulse at the 5-ms duration. In fact, at short enough time scales when heat diffusion is minimal (on the order of 1-ms pulses), the optimum beam shape is predicted to be the original top hat shape. However, the therapeutic window at 1-2 ms for a top hat beam is known to be too low for safe operation, so the 50% and 75% modulation beams were used to study potential improvement between 2-50 ms pulse durations.

2.4 *Temporal Modulation of Laser Power*

Similarly, modification of the temporal profile of a laser beam exposure can also aid in homogenizing the temperature profile of the target. A conventional "flat" laser pulse will deposit heat linearly with time during exposure. Due to 3-dimensional heat diffusion along the temperature gradient, this causes the center of the targeted spot to experience a gradual rise in temperature approaching an elevated steady state. Because of the exponential dependence of Arrhenius damage on temperature (Equation 2), the majority of the clinical effect is achieved in only the last 25% of the exposure, as shown in Figure 7a.

a)

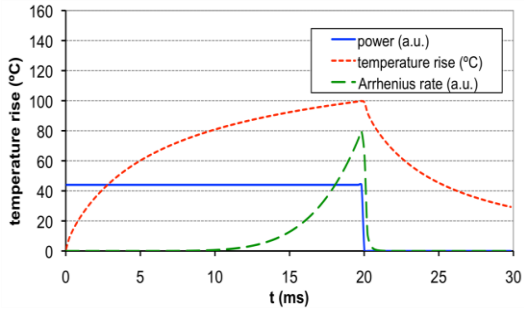

b)

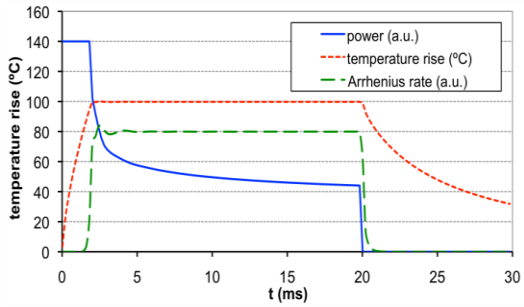

Figure 7. Temporal optimization: temperature rise (red) and Arrhenius rate (green) corresponding to (a) a conventional pulse and (b) a pulse with temporal shaping. The area under the green curves correspond to total incurred tissue damage.

However, the input pulse can easily be shaped to improve the resulting temporal profile, better utilizing the full duration of the pulse. One example of such a shaped pulse is given in Figure 7b, in which the temperature quickly reaches its peak and is held constant for 90% of the pulse duration. Thus, the Arrhenius rate contributes significantly for 90% rather than 25% of the pulse. Because the total area under the Arrhenius rate curve does not need to increase for a minimally effective lesion, the same clinical result can be achieved with a lesser peak temperature elevation in the RPE

cells. This, in turn, should allow for a greater therapeutic window, as it diminishes the likelihood of the peak temperature crossing the water vaporization threshold during exposure.

3. Experimental

All experiments pertaining to this study were performed in the Hansen Experimental Physics Laboratory and the Stanford Medical Center at Stanford University in Stanford, CA between June 2008 and April 2010.

3.1 *Biological Model: Dutch Belted Rabbit*

Dutch Belted rabbits were chosen as the biological model for this study because of their characteristically large eyes, their relatively uniform retinal pigmentation, and for ease of handling and follow-up. Compared with New Zealand White rabbits, another common model in ophthalmological studies, Dutch Belted rabbits have also been shown[15] to have a clearer surgical anatomy, allowing for improved accuracy in evaluation of retinal lesions post-exposure.

3.2 *Control: Conventional Spatial and Temporal Profile*

For the control in these experiments, a PASCAL photocoagulator (Optimedica, Santa Clara, CA) was used as the surgical implement. The output radiation of PASCAL is a 532-nm wavelength continuous wave (CW) beam with delivery through a 200-µm optic fiber. The in-air spot size was characterized to have a 200-µm diameter and a 20-µm 10-90% transition. Power was applied as a square pulse in time.

3.3 *Ring Beam*

To mimic the PASCAL system, a 532-nm CW frequency-doubled ND-Yag pumped diode laser (85-GHS-305, Melles Griot) was coupled into a 200 µm multimode fiber for delivery onto the target by means of a modified slit lamp (Figure 8).

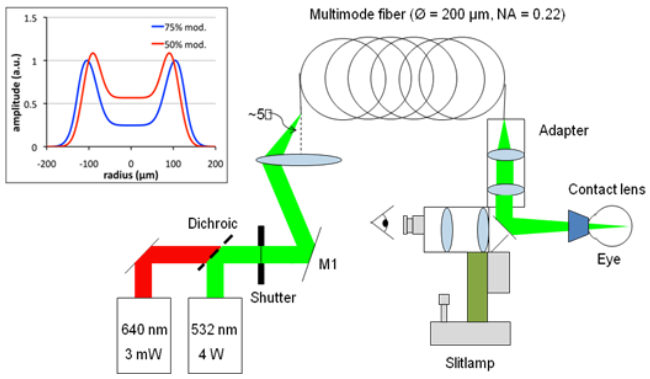

Figure 8. Experimental schematic for ring beam. Adjustment of incident angle on fiber allows for change in depth of ring modulation (inset).

To produce a ring-shaped cross-section, the laser beam was coupled into this fiber at an incident angle of approximately 5° to utilize the first higher-order (TEM01*) transmission mode of the fiber, which gave a maximum modulation of approximately 90% between the center and

the peak of the intensity profile as characterized on CCD (Figure 9).

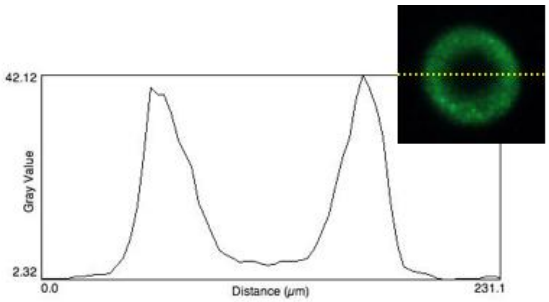

Figure 9. Cross-sectional intensity characterization of sample ring beam with 90% center-to-peak modulation, as imaged on CCD camera (inset).

Experimental beams with less pronounced modulation (75% and 50% rather than 90%) were also produced by variation about this incident angle, and were characterized in the same manner. These beam modulations were chosen because of the computational model's projections of increased therapeutic window at pulse durations of 5-10 ms (Figures 6a-c) for beams with such levels of modulation, as discussed in section 2.3 above.

3.4 *Temporally Modulated Pulse*

An optimization algorithm was combined with the computational model to determine a pulse shape that would maximize the therapeutic window of a given pulse duration. Optimal curve fitting was found to be dependent on the duration of the pulse; as such, different waveforms were used for the 5-ms, 10-ms, and 20-ms pulses tested. For each case, the curve obtained was characterized by a constant, high initial power followed by an exponential decrease to a lower power. As discussed in section 2.2, the intended effect of this was to maintain a constant peak temperature once reached (Figure 7b).

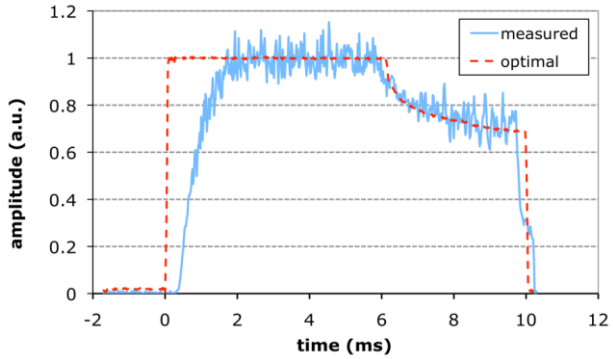

Figure 10: Sample characterization of shaped pulse, compared to ideal. The rise time of the laser (600 μs) was noticeable at short pulse durations.

The experimental temporally modulated pulse was generated with the use of a modified PASCAL system driven by an arbitrary function generator (33120A, Agilent, Santa Clara, CA). Pre-defined shapes for the pulse were loaded onto a custom computer interface (LabView, National Instruments, Austin, TX), which output the waveform to the function generator, allowing the various pulse shapes to be tested. Characterization of this temporal shaping (Figure 10) showed a close correspondence with the ideal input curve with the exception of the first 2 ms of each pulse, where the rise time of the laser (600 μs) caused noticeable deviation from the input curve. The pulse shape

optimization algorithm did not take into account this nonzero rise time due to complexity of computation.

3.5 *Power Titration and Ophthalmic Severity Rating*

To experimentally validate the results of the computational modeling, measurements of therapeutic window were taken at 2-50 ms pulse durations by comparing the power required to produce rupture to the power required to produce a lesion characterized as "minimally visible" on the ophthalmic scale. Peak power thresholds of retinal coagulation and rupture were measured in 22 Dutch Belted rabbits *in vivo* to yield therapeutic window measurements. One of two graders rated each lesion 3 seconds after exposure on the following scale of increasing intensity: invisible, barely visible, mild, intense, rupture. For the control and ring beam measurements, the constant input power on the laser was used as the nominal value for data analysis, whereas the peak power of the temporally shaped pulse was used for the same purpose. Power was titrated to find the minimum required power on average to produce a rupture lesion and a barely visible lesion. The therapeutic window was then found by taking the ratio of these average thresholds at each pulse duration.

3.6 *Fluorescence Live/Dead Assays*

Calcein AM/Propidium Iodide fluorescence viability assay (C1430, Invitrogen) was used to assess damage zone size and character in porcine RPE samples (Figure 11). This characterization was used to compare the relative size of treatment area between using a conventional and a ring beam, as it was noted that coupling into the ring mode of the optic fiber tended to slightly enlarge the cross-sectional size of the laser beam (cf. Figure 4a-c).

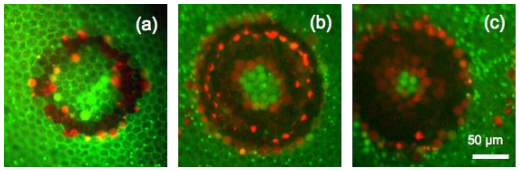

Figure 11. Calcein/PI fluorescent micrograph of ring-beam exposures on RPE sheet with a pulse duration of 10 ms. Laser power is (a) 30 mW, (b) 40 mW and (c) 50 mW. Filling in of the center of the lesion is visible at higher powers.

4. Findings

4.1 *Ring Beam*

For the control beam as well as for the 50% and 75% modulation ring beams, power required to produce all types of lesions increased with decreasing pulse duration (Figure 12a), and therapeutic window decreased logarithmically with decreasing pulse duration (Figure 12b), as observed in previous studies with conventionally-shaped beams[16]. However,

although the computational model predicted that the 75% modulated beam should have a higher TW than either the control or the 50% modulation beam at all durations 2-50 ms, the experimental results showed the greatest improvement in average TW occurred for the 50% beam for durations 2-20 ms (Figure 13). Statistically significant improvement in TW ($p<.05$) was noted for the 10- and 20-ms pulse durations for both trial beams, and also in 50-ms pulses for the 75% modulation beam.

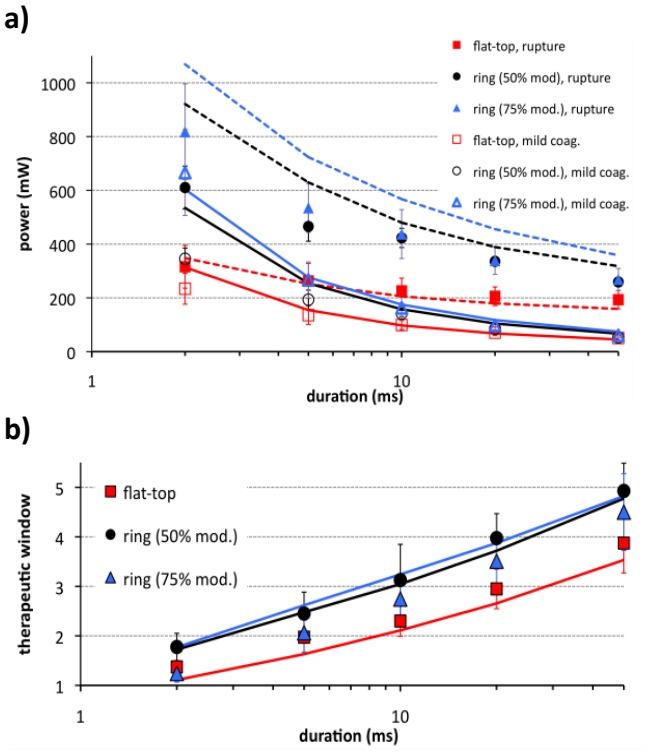

Figure 12. (a) Computed coagulation and rupture thresholds (line) along with measured thresholds (symbol) for flat-top beam (red), 50%-modulated ring-beam (black), and 75%-modulated ring-beam (blue) as a function of pulse duration. (b) Computed safe therapeutic window (line) with measured data (symbols) as a function of pulse duration.

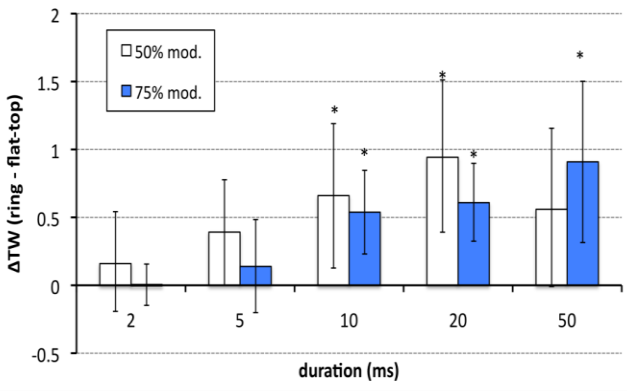

Figure 13. Experimentally observed change in TW for ring beams with 50% and 75% modulation. Improvement is statistically significant ($p<.05$) where indicated (*).

Maximum TW at the 10-ms duration was observed with the 50% modulation beam, with a mean value slightly greater than 3.

4.2 *Temporally Modulated Pulse*

As with the ring beam measurements, the peak power required to produce lesions of any intensity increased with decreasing pulse duration, and the therapeutic window was observed to decrease with decreasing pulse duration for both the conventional and the shaped pulse beams. Computational predictions of threshold power to produce both rupture and minimally effective lesions agreed remarkably well with experimental observation (Figure 14a). Observed TW resulting from these measurements was found to improve to an even greater degree than predicted for 5-ms and 10-ms durations (Figure 14b). Improvement was shown to be statistically significant ($p<.05$) for

these durations, while the slight difference in TW for the 20-ms duration was not (p=.28).

a)

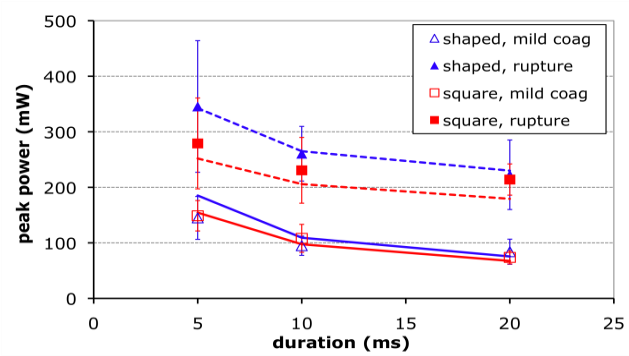

b)

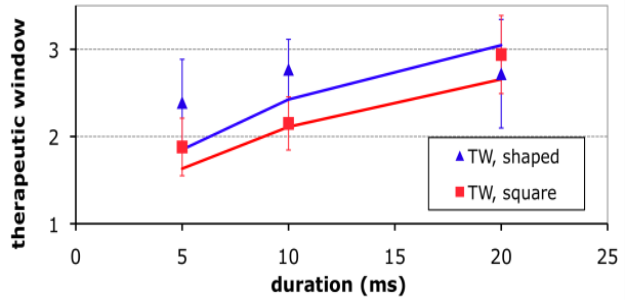

Figure 14. (a) Computed coagulation and rupture thresholds (line) along with measured thresholds (symbol) for modulated pulse (blue) and square pulse (red) as a function of pulse duration. (b) Computed safe therapeutic window (line) with measured data (symbols) as a function of pulse duration.

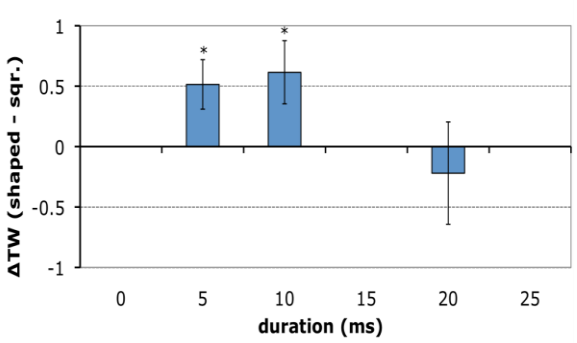

Figure 15. Experimentally observed change in therapeutic window for temporally shaped pulse over a conventional (square) beam. Findings are statistically significant where indicated (*).

The improved TW for the shaped was measured to be approximately 2.3 at the 5-ms pulse duration, and approximately 2.8 at 10 ms.

5. Discussion

The hypotheses of this study were threefold:

1. Retinal photocoagulation can be rendered safer at shorter pulse durations by optimizing the thermodynamic profile of the treatment, as implied by the Arrhenius damage model.

2. Spatial or temporal shaping of the incident laser pulse can heat a target region more uniformly.

3. Such spatially or temporally shaped beams will yield clinical benefit in accordance with hypothesis (1).

As hypothesis (1) is particularly difficult to test directly, the combination of computational modeling and experimental verification of hypothesis (3) was used in this study to provide indirect evidence to the validity of the Arrhenius damage model. However, the observed success of this indirect evidence is striking. By thermal modeling, two simple yet essentially orthogonal methods of homogenizing the thermal profile of a photocoagulation pulse were identified; each method was tested separately and found to yield statistically significant improvement in therapeutic window, as predicted.

Of the two shaping methods (spatial and temporal), spatial shaping with 75% modulation was predicted by the computational model to yield a greater benefit in the therapeutic window for 10-ms pulse durations. Experimentally, the spatially-shaped beam was shown to be the most effective; however, the 50% modulation showed greater improvement than the 75% beam at all durations below 50 ms, contrary to expectation. It was also the only beam studied which raised the therapeutic window to at least 3 at the 10-ms duration.

If clinical trials with human patients also prove successful to a similar degree, practical implementation in a "next-generation" PASCAL system would likely be simpler for a temporally shaped beam, since the only modifications necessary would be in the computer driving the laser. Unfortunately, the specific waveform implemented in this study only improved the TW at the 10-ms pulse duration up to 2.8, not quite rendering it acceptable for clinical use at this speed. However, there is potential for further improvement on this method by incorporating the delayed rise time of the laser into the calculation of optimal waveforms. Without taking this explicitly into account in the waveform calculation, essentially a shorter pulse than necessary was used. Incorporating this discrepancy between desired and actual pulse output into the optimization algorithm should yield a more pronounced TW increase at shorter pulse durations, since the rise time is essentially constant as the total pulse duration decreases, causing a greater percentage of the pulse to not behave as desired.

Possibilities for future work also include investigating the potential for combining both trial methods explored in this study. A full optimization of both the spatial and the temporal temperature profiles could potentially achieve safe clinical operation for 5-ms pulses or possibly even shorter durations. Each of the modifications studied here separately increased the therapeutic window in the 5-ms regime to nearly 3; it is not difficult to believe that

if combined, the two methods could yield sufficient TW increase to render surgery even at this short duration safe.

References

[1] Campbell C J et al., Clinical studies in laser photocoagulation, *Arch. Ophthalmol*. **74** 57 (1965)
[2] J. Spranger et al., *Diabetologia*, **43** (11), 1404 (2000)
[3] V.-P. Gabel, R. Birngruber, and F. Hillenkamp, Die lichtabsorption am augenhintergrund. *Gesellschaft für Strahlen- und Umweltforsch*, GSF-Bericht A55 (1976).
[4] Blumenkranz, M.S., et. al., Semiautomated patterned scanning laser for retinal photocoagulation. *Retina*, 2006. 26(3): p. 370-376.
[5] J. Weiter, F. Delori, G. Wing, and K. Fitch, Retinal pigment epithelial lipofuscin and melanin and choroidal melanin in human eyes. *Invest. Ophthalmol. Visual Sci.* **27**(2), 145–152 (1986).
[6] S. Schmidt and R. Peisch, Melanin concentration in normal human retinal pigment epithelium, regional variation and age-related reduction. *Invest. Ophthalmol. Visual Sci.* **27**(7), 1063–1067 (1986).
[7] P. W. Lappin and P. S. Coogan, Relative sensitivity of various areasof the retina to laser radiation. *Arch. Ophthalmol. (Chicago)* **84**(3),350–354 (1970).
[8] Jain A., et. al., The effect of pulse duration on the size and character of the lesion in retinal photocoagulation. *Arch. Ophthalmol*., 2008. 126(1): p. 78-85.
[9] Gerstman B, et. al., Laser induced bubble formation in the retina. *Lasers in Surgery and Medicine*, 1996. 18:10-21
[10] Sramek, C. et. al., Dynamics of retinal photocoagulation and rupture. *J. Biomed. Opt*., 2009. 14(3): 034007
[11] Walter A. Strauss, *Partial Differential Equations*, 2nd ed., (Wiley, Hoboken, NJ, 2008) p. 67
[12] D. M. Simanovskii, M. A. Mackanos, A. R. Irani, C. E. O'Connell-Rodwell, C. H. Contag, H. A. Schwettman, and D. V. Palanker, Cellular tolerance to pulsed hyperthermia. *Phys. Rev. E* **74**(1 Pt 1), 011915 (2006).
[13] M. Niemz, *Laser-Tissue Interactions. Fundamentals and Applications*, Springer, Berlin (2002).
[14] Bhowmick S, Coad JE, Swanlund DJ, Bischof JC. In vitro thermal therapy of AT-1 Dunning prostate tumours. *International Journal of Hyperthermia* 2004;20:73-92.

[15] Q. H. Nguyen et al., Comparison of New Zealand White versus Dutch Belted Rabbits as a Model for Glaucoma Surgery. *Invest Ophthalmol Vis Sci* 2002;43: E-Abstract 3335.
[16] Jain A., et. al., The effect of pulse duration on the size and character of the lesion in retinal photocoagulation. *Arch. Ophthalmol*., 2008. 126(1): p. 78-85.